

# Temperature-Dependent Reinforcement of Hydrophilic Rubber Using Ice Crystals

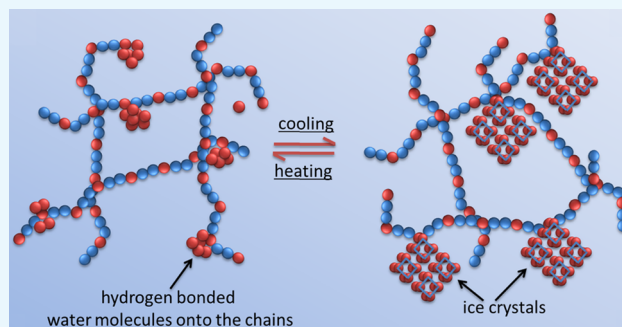
Tamil Selvan Natarajan,<sup>†,‡</sup> Klaus Werner Stöckelhuber,<sup>\*,†,§</sup> Mikhail Malanin,<sup>†</sup> Klaus-Jochen Eichhorn,<sup>†</sup> Petr Formanek,<sup>†</sup> Uta Reuter,<sup>†</sup> Sven Wießner,<sup>†,‡</sup> Gert Heinrich,<sup>†,‡</sup> and Amit Das<sup>†,§,¶</sup>

<sup>†</sup>Leibniz-Institut für Polymerforschung Dresden e. V., Hohe Straße 6, D-01069 Dresden, Germany

<sup>‡</sup>Technische Universität Dresden, Institut für Werkstoffwissenschaft, D-01062 Dresden, Germany

<sup>§</sup>Technical University of Tampere, Korkeakoulunkatu 16, Fi-33720 Tampere, Finland

**ABSTRACT:** This is the first study on the impact of ice crystals on glass transition and mechanical behavior of soft cross-linked elastomers. A hydrophilic elastomer such as epichlorohydrin–ethylene oxide–allyl glycidyl ether can absorb about ~40 wt % of water. The water-swollen cross-linked network exhibits elastic properties with more than 1500% stretchability at room temperature. Coincidentally, the phase transition of water into solid ice crystals inside of the composites allows the reinforcement of the soft elastomer mechanically at lower temperatures. Young's modulus of the composites measured at  $-20\text{ }^{\circ}\text{C}$  remarkably increased from 1.45 to 3.14 MPa, whereas at  $+20\text{ }^{\circ}\text{C}$ , the effect was opposite and the Young's modulus decreased from 0.6 to 0.03 MPa after 20 days of water treatment. It was found that a part of the absorbed water, ~74% of the total absorbed water, is freezable and occupies nearly 26 vol % of the composites. Simultaneously, these solid ice crystals are found to be acting as a reinforcing filler at lower temperatures. The size of these ice crystals is distributed in a relatively narrow range of 400–600 nm. The storage modulus ( $E'$ ) of the ice crystal-filled composites increased from 3 to 13 MPa at  $-20\text{ }^{\circ}\text{C}$ . The glass transition temperature ( $-37\text{ }^{\circ}\text{C}$ ) of the soft cross-linked elastomer was not altered by the absorption of water. However, a special transition (melting of ice) occurred at temperatures close to  $0\text{ }^{\circ}\text{C}$  as observed in the dynamic mechanical analysis of the water-swollen elastomers. The direct polymer/filler (ice crystals) interaction was demonstrated by strain sweep experiments and investigated using Fourier transform infrared spectroscopy. This type of cross-linked rubber could be integrated into a smart rubber application such as in adaptable mechanics, where the stiffness of the rubber can be altered as a function of temperature without affecting the mechanical stretchability either below or above  $0\text{ }^{\circ}\text{C}$  (above the glass temperature region) of the rubber.



## INTRODUCTION

Fillers are small, often nanoscaled, solid particles that are incorporated into soft elastomers mainly to increase the mechanical and other engineering properties such as modulus, hardness, tensile strength, abrasion, tear, fatigue, and crack resistance, leading to better performance and a longer lifetime of the final rubber product. More specifically, carbon black and precipitated silica are the main reinforcing fillers<sup>1</sup> used in rubber for different technological applications, especially in the tire industry. Reinforcement of elastomer composites by fillers is primarily influenced by the particle size, aspect ratio, surface area, and structure of the fillers. In short, it can be said that reinforcement of the elastomers depends on the ability of the polymer chains to transfer the load to the filler matrix. The mechanism of reinforcement has been debated for a long period of time, and several theories have been proposed.<sup>2</sup>

Hydrophilic polymers are increasingly used in the field of sensors (humidity and glucose), membranes, coatings (anti-fouling and antifogging), caulking, body implants, adsorbents, mechanical actuators, and various smart materials.<sup>3,4</sup> In general, hydrophilic polymers swell in water to a certain extent (increase

in size and shape). The absorbed water may lead to major changes in the mechanical and chemical properties, which depend on the type of polymer, the degree of swelling, and so forth. Blasi et al.<sup>5</sup> report that a small amount of water absorbed by poly-(D,L-lactide-co-glycolide) under high relative humidity acts as a plasticizer, lowering the glass transition temperature  $T_g$  of the polymer proportional to the amount of water in the matrix. Ito et al.<sup>6</sup> found that epoxy resins showed a significant decrease in elastic modulus proportional to the degree of water sorption. Water absorbed in a hydrophilic polymer presents thermodynamic properties slightly different from those of water in the bulk liquid phase.<sup>7</sup> Tanaka et al.<sup>8</sup> classify the hydrated water in a polymer into three types: *nonfreezable bound water*, *freezable bound water* (also called *intermediate water*), and *free water*. Initially, the water molecules get isolated, are homogeneously distributed throughout the polymer, and have greater restricted mobility because they strongly interact with

**Received:** November 30, 2016

**Accepted:** January 18, 2017

**Published:** February 2, 2017

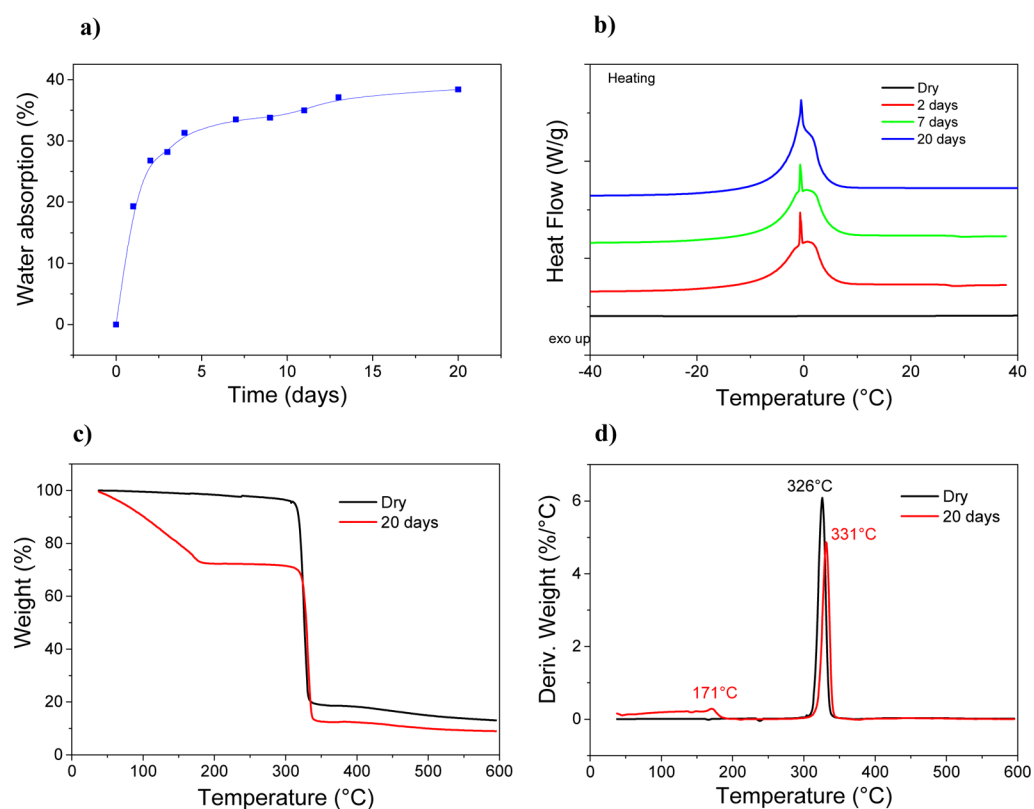


**Figure 1.** (a) Water absorption characteristics of cross-linked GECCO, (b) differential scanning calorimetric study of the dry cross-linked GECCO and cross-linked GECCO samples swollen in water for different days, (c) thermogravimetric analysis of dry and 20-day water-swollen elastomers, and (d) derivative weight of the composite as a function of temperature during the thermogravimetric analysis.

the polar groups in the polymer chain, called *nonfreezable bound water*. After a certain threshold of bound water is reached, the additional water molecules interact weakly with the hydrophilic groups of the polymer and are termed *freezable bound water*. Furthermore, when the amount of absorbed water increases, it remains isolated and is termed *free water*. Only the free water and freezable bound water form ice crystals when cooled down. They differ in the melting point: the crystals of free water melt at 0 °C, whereas the ice crystals of freezable bound water melt at temperatures lower than 0 °C.<sup>9</sup> Bjerrum<sup>10</sup> states that ice crystals can be present in two closely related crystal structures: hexagonal and cubic ice crystals. A hexagonal crystal structure is obtained by freezing the water slowly, whereas the cubic structure is normally formed by depositing vapor at low temperatures. The hexagonal crystal structure is the common form of ice crystals, owing to its tetrahedral molecular geometry. Kumai<sup>11</sup> reports that the ice crystal structure depends on the temperature of substrates. The hexagonal form of ice crystals is formed below −100 °C; between −100 and −130 °C, both the hexagonal and the cubic forms of ice can be found; and above −130 °C, only cubic ice crystals were detected.

In this paper, we investigate the impact of imbibed water on the mechanical and dynamic mechanical behaviors of soft cross-linked elastomer composites at low temperatures, particularly when the water molecules remain in a nanoconfined and frozen state. A cross-linked hydrophilic polymer, epichlorohydrin–ethylene oxide–allyl glycidyl ether (GECCO), was used as an elastomeric matrix. The GECCO elastomer absorbs water, which can be transformed into ice crystals after cooling down to lower temperatures. We performed detailed studies to understand the

reinforcing ability of the frozen ice in the soft rubber matrix. Studies on the in situ formation of ice crystals, their nanoconfinement structures, and their direct interaction with GECCO are the main issues discussed in this article. Additionally, this paper deals with the effect of ice crystals on the dynamic mechanical and quasistatic mechanical behaviors of the soft elastomer.

## RESULTS AND DISCUSSION

Water absorption characteristics of the GECCO composites are shown in Figure 1a. GECCO composites absorb water of about ~40% of the weight of the dry sample and reach 90% of their swelling capacity in 4–5 days. GECCO, being a polymer with oxygen atoms in the polymer backbone, is very hydrophilic, and in its cross-linked state, it can absorb a considerable amount of water. A certain amount of this absorbed water can be frozen into ice crystals, when the matrix material is cooled down at temperatures below 0 °C. The amount of freezable and nonfreezable water can be calculated using the differential scanning calorimetry (DSC) with the help of endothermic ice-melting profile of the swollen cross-linked elastomer.<sup>12</sup> The heating curves of the dry elastomers and 2-, 7-, and 20-day water-swollen elastomers are shown in Figure 1b. The broad endothermic peak is due to the convergence of the melting of free water and freezable bound water.<sup>13</sup>

So, we can assume that the *total water content* ( $W_t$ ) is the sum of *nonfreezable water content* ( $W_{nf}$ ) and *freezable water content* ( $W_f$ ). The freezable water content ( $W_f$ ) subsumes here the freezable water fractions of free and freezable bound water in the polymer.

$$W_t = W_{nf} + W_f \quad (1)$$

Assuming equal melting enthalpies for the different types of water (free and freezable bound water), the amount of freezable water can be obtained from the following equation

$$\frac{W_f}{W_d} = Q \frac{\Delta H_s}{\Delta H} \quad (2)$$

where  $W_d$  is the weight of the dry sample,  $W_s$  is the weight of the swollen elastomer,  $\Delta H_s$  is the enthalpy of the swollen elastomer, and  $\Delta H$  is the enthalpy of bulk water, which can be taken as  $\sim 330$  J/g [the melting enthalpies of different ice crystals are not considered in this calculation, and so, the maximum error in the calculated amount of freezable water/ice crystals was expected to be less than 5%<sup>9</sup> (lowest for tetragonal ice crystals, 312 J/g, and highest for hexagonal ice crystals, 334 J/g)].

The swelling ratio  $Q$  can be written as

$$Q = \frac{W_s}{W_d} \quad (3)$$

Similarly, the amount of nonfreezable water can be obtained using

$$\frac{W_{nf}}{W_d} = Q \left( W_g - \frac{\Delta H_s}{\Delta H} \right) \quad (4)$$

where

$$W_g = \frac{W_t}{W_s} = \frac{Q - 1}{Q} \quad (5)$$

The ice-melting enthalpies ( $\Delta H_s$ ) were obtained by integration of the peak areas of the DSC curves (Figure 1b) of water-swollen GECO composites. The weight percentage (wt %) of the freezable water and the volume percentage (vol %) of the ice crystals formed in the GECO composite are shown in Table 1.

**Table 1. DSC Melting Profile and Volume Percentage of the Filler (Ice Crystals) Formed in GECO Composites**

water absorption time	absorbed water ( $W_f/W_s$ ) (wt %)	$\Delta H$ (J/g)	freezable water ( $W_f/W_t$ ) (%)	vol % of the ice crystals that act as filler in GECO composites
GECO (dry)				
2 days	20.5	56.7	81.6	21.2
7 days	25.4	61.5	73.2	23.7
20 days	28	66.3	74.2	25.4

1. The vol % of the ice crystals with respect to the total volume of the composite was calculated using

$$\begin{aligned} & \text{Vol \% of the filler} \\ &= \frac{\text{vol of freezable water}}{\text{vol of dry composite} + \text{vol of total absorbed water}} \\ & \times 100 \end{aligned} \quad (6)$$

From Table 1, it can be seen that with an increase in the absorbed water inside of the rubber, the vol % of the ice crystals steadily increases, indicating more freezable water molecules with a higher amount of absorbed water. A maximum of  $\sim 26$  vol % of ice crystals was obtained, and it was also found that

70–80% of the absorbed water molecules is available for the formation of ice crystals.

From the thermogravimetric analysis, it was found that the 20-day water-swollen elastomers undergo a two-stage degradation process (Figure 1c). The first degradation is due to the evaporation of water and low-molecular-weight cross-linking ingredients. The second stage appears due to the polymer degradation. At 180 °C, the first degradation process is completed with a degradation loss of 26 wt %. This is in accordance with the swelling studies, where an amount of absorbed water of 28 wt % can also be found (Table 1). It can be noted from the derivative plot (Figure 1d) that the maximum degradation peak of the polymer chain itself is shifted from 326 to 331 °C, indicating a more stable compound after treatment with water.

Cryo-transmission electron microscopy (cryo-TEM) is used for imaging frozen-hydrated specimens at cryogenic temperatures.<sup>14</sup> In this work, the solid ice crystals at freezing temperatures in swollen GECO composites were visualized using cryo-TEM. The cryo-TEM images of 20-day water-swollen GECO composites are shown in Figure 2. Hereby, it can be observed roughly that spherical- to oval-shaped ice crystals are uniformly distributed in the matrix. The black regions are ice crystals condensed from air humidity at the surface of the specimen. Energy-filtered transmission electron microscopy (EFTEM) technique was additionally used to deduce the chemical composition of the imaged composite. Elemental maps of carbon and oxygen from these EFTEM measurements are shown in Figure 2b. The green and red areas indicate the presence of carbon in the polymer and the presence of oxygen in solid ice ( $H_2O$ ), respectively. The presence of oxygen in the GECO polymer is also identified, as red dots in the green areas. The oxygen-enriched domains (red) confirm the formation of solid ice crystals. The particle size of these ice crystals remains in the range of submicron level (400–600 nm), which may act as reinforcing filler particles in swollen GECO composites at low temperatures. Water-swollen GECO composites were in situ freeze-dried during cryo-TEM imaging (see Figure 2c). During the freeze-drying process, ice crystals inside of the specimen sublimated and left small holes (pores) in the composites. These pores in the composites confirm the presence of ice crystals inside of the composite before freeze-drying. Selected-area electron diffraction (SAED) pattern of water-swollen GECO composites yielded a ring and spot pattern, matching those expected for the polycrystalline ice crystals (Figure 2d). SAED pattern can be indexed as (002), (101), (102), (103), and (201) planes, which confirm the hexagonal crystal structure of ice, in accordance with ref 11 (Table in Figure 2).

The dynamic mechanical behavior of water-filled cross-linked GECO composites was also studied. The loss factor  $\tan \delta$  as a function of temperature is shown in Figure 3a. The glass transition temperature ( $T_g$ ) of the elastomer was found to be at  $-37$  °C under the experimental dynamic conditions at 10 Hz frequency.  $T_g$  is found to be unaltered with different water contents of the elastomer (elastomers swollen for different days). The unaltered glass transition temperature of elastomers swollen for different days confirms the formation of ice crystals and the absence of plasticizing effect. The interaction of ice crystals with the polymer chains can be seen from reduction in the  $\tan \delta$  peak height. A strong dependency on the  $\tan \delta$  peak height was noticed with a higher amount of water. Simultaneously with an increase in the water content, the

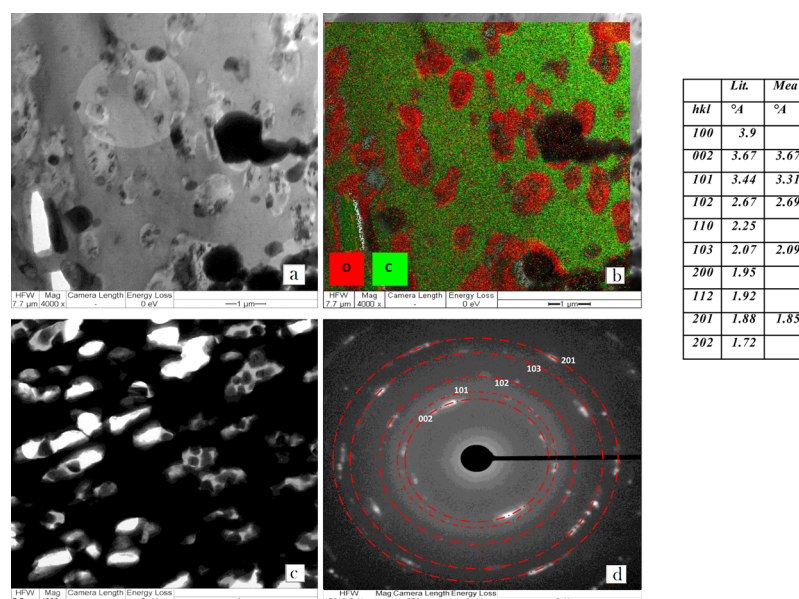


**Figure 2.** (a) Formation of ice crystals can be seen in cryo-TEM image of water-swollen GECO composites, (b) carbon and oxygen maps overlaid on (a), (c) pores and voids produced by freeze-drying in situ in cryo-TEM, and (d) SAED image of GECO–ice crystal composites. The indexed rings correspond to the crystalline lattice of hexagonal ice crystals in accordance with the literature (see inserted Table).

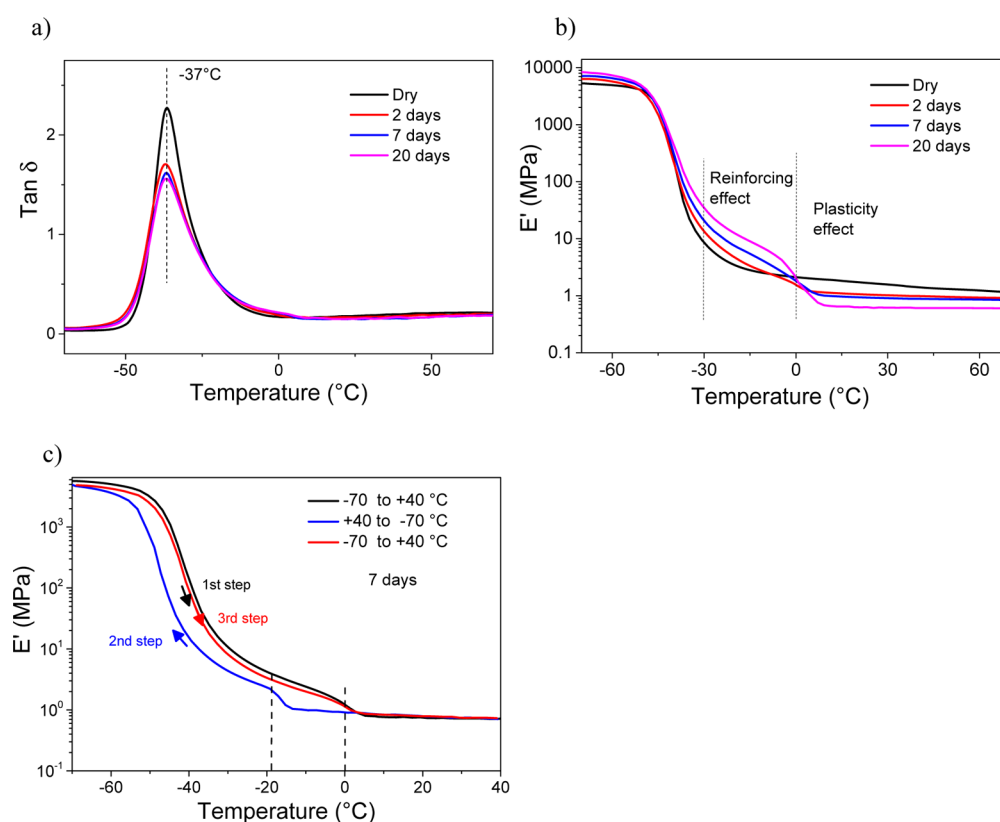


**Figure 3.** (a) Mechanical loss factor  $\tan \delta$ , (b) storage modulus  $E'$  as a function of temperature of GECO composites water-swollen for different times, and (c) cyclic temperature sweep experiment with 7-day water-swollen elastomers.

storage modulus increases in the temperature range of  $-37$  to  $0$  °C (Figure 3b). The storage moduli at  $-20$  °C of 2-, 7-, and 20-day-swollen GECO composites are about 40% (5 MPa), 123% (8 MPa), and 271% (13 MPa) higher than those of the pure GECO composites without water (3 MPa). The solid ice is expected to interact with polymer chains by hydrogen bonding between the hydroxyl groups of the ice crystals and the oxygen

in the polymer chains. Owing to a direct interaction of the rubber and the solid ice, the ice crystals behave as a reinforcing filler, which might be the primary reason for the enhanced storage modulus. It should be mentioned here that the composite with less water content ( $\sim 5$  wt % of the water content), did not show any improvement of in the storage modulus (not shown here) because of an insufficient quantity

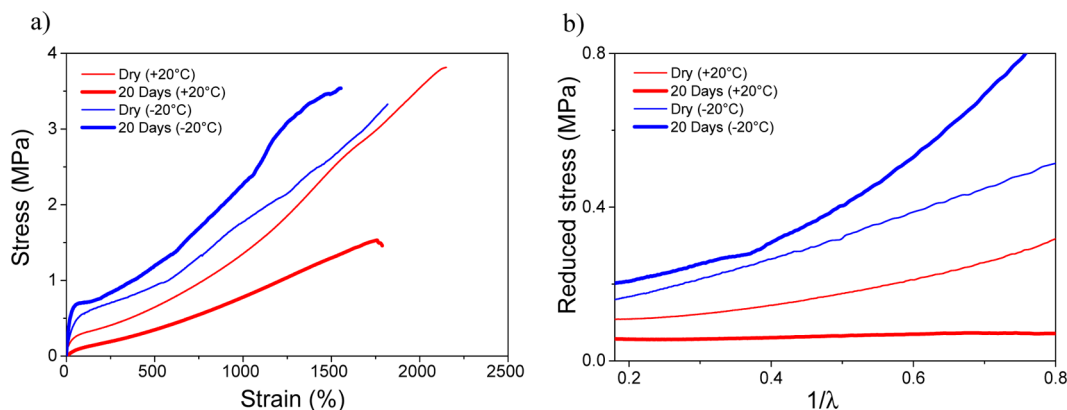


**Figure 4.** (a) Stress–strain properties of dry and 20-day water-swollen elastomers. The experiment was performed at  $-20$  and  $+20$  °C. (b) MR plot of the dry and 20-day water-swollen GECO composites.

of free water molecules, which cannot be transformed into ice crystals.

At  $0$  °C, a crossover point in the storage modulus can be observed (Figure 3b); the reinforcing behavior of the ice crystals is now replaced by a plasticizing effect of the water inside of the rubber. The storage moduli at  $+20$  °C of 2-, 7-, and 20-day water-swollen GECO composites are about 41% (1 MPa), 45% (0.94 MPa), and 63% (0.62 MPa) lower than those of the pure GECO composites without water (1.7 MPa).

To understand this reversible transformation of water into ice crystals, a cyclic temperature sweep was carried out with 7-day water-swollen elastomers (Figure 3d). In the first heating step, the storage modulus of the compound continuously decreases, until it reaches a plateau value around  $0$  °C. In the cooling cycle, this rubbery plateau can be observed up to  $-14$  °C, and then the storage modulus increases.

Similar shifts in temperature (difference in the melting and freezing temperatures of water has been reported in DSC) can be seen elsewhere.<sup>15</sup> Most probably, the observed hysteresis is due to the poor thermal conductivity of the rubber and a slow ice crystal formation of the absorbed water. In the second heating step, the curve follows that of the first heating cycle, which indicates a reversible temperature-dependent mechanical performance of the rubber sample.

The impact of pressure-induced melting during DMA experiments (static and dynamic strains applied repetitively) has been analyzed, considering the phase diagram of water  $dP/dT \approx -13.5$  MPa/K near  $0$  °C and 1 atm ( $\sim 0.1$  MPa). Pressure changes can be roughly estimated with changes in the modulus in the corresponding region of the temperature change. According to Figure 3c, roughly  $\Delta p \approx \Delta E' \approx 1$  MPa (or even smaller) has been obtained in a sensitive temperature range between  $-20$  and  $0$  °C, resulting in an expected temperature change  $|\Delta T| \approx 0.07$  K or even smaller.<sup>16,17</sup> The temperature changes were found to be very less, and so, such an effect (pressure-induced melting) has been neglected in this work.

To summarize the detailed observation in Figure 3, the glass transition temperature of rubber was found to be  $-37$  °C (10 Hz DMA measurement); in the temperature range from  $-37$  to  $0$  °C, the ice crystals formed reinforced the rubber; above  $0$  °C, the mechanical properties are drastically changed toward a soft rubber, where the water content is acting as a softening agent.

Stress–strain studies were carried out at  $-20$  °C and at room temperature (RT) ( $+20$  °C); the results are shown in Figure 4a.

For water-swollen elastomers, the sample was kept at  $-20$  °C for 30 min (20-day water-swollen) before stress–strain measurements. The water-swollen elastomers show higher mechanical properties at  $-20$  °C than the dry GECO sample. The stress at 100% strain (100% modulus, M100) values increases from 0.55 to 0.71 MPa compared with the dry sample. However, at RT ( $20$  °C), the water-containing composites show poor mechanical properties, and the M100 value drops from 0.32 to 0.11 MPa. However, still all composites show more than 1500% stretchability. This confirms the plasticizing effect of water on the hydrophilic matrix (GECO). On the other hand, a stronger mechanical performance of the water-swollen elastomer at  $-20$  °C indicates the reinforcing action of solid ice crystals and their direct interaction with the polymer chains by hydrogen bonding. The volume fraction of the ice crystals acting as filler particles was calculated using the initial modulus derived from the stress–strain experiment evaluated at  $-20$  °C with the help of hydrodynamic reinforcement effect.

The hydrodynamic reinforcement factor can be estimated by the Chen and Acrivos equation for hard spherical particles<sup>18,19</sup>

$$E/E_0 = 1 + 2.5\phi + 5.0\phi^2 \quad (7)$$

Here,  $E$  is the initial modulus of water-swollen elastomers,  $E_0$  is the initial modulus of the dry sample, and  $\phi$  is the volume fraction of the ice crystals formed. The initial modulus of the dry sample was 1.45 MPa, and the value for 20-day water-swollen elastomers was 3.14 MPa. The volume fraction of ice crystals present inside of the cross-linked GECO composites was found to be 29 vol %, which is well consistent with the results of the DSC study ( $\sim 26$  vol %).

The filler reinforcement and filler/polymer affinity can be analyzed from the stress–strain behavior illustrated by a phenomenological expression proposed by Mooney and Rivlin<sup>20–22</sup>

$$\frac{\sigma}{\lambda - \lambda^{-2}} = 2(C_1 + C_2\lambda^{-1}) \quad (8)$$

where  $\sigma$  is the applied stress,  $\lambda$  is the extension ratio, and  $C_1$  and  $C_2$  are the Mooney–Rivlin (MR) constants. The plot obtained from the reduced stress ( $\sigma/(\lambda - \lambda^{-2})$ ) against  $1/\lambda$  and the analysis of linear regimes in the plot provided the values of  $C_1$  (intercept) and  $C_2$  (slope). The MR plots for dry and water-swollen elastomers are shown in Figure 4b. Furthermore, cross-link density ( $\nu$ ) can be calculated from  $C_1$  using the expression  $2C_1 = \nu kT$ , where  $\nu$  is the cross-link density,  $k$  is the Boltzmann

constant, and  $T$  is the absolute temperature. A slight decrease in the cross-link density of the water-swollen elastomer at 20 °C and a certain degree of increased value at -20 °C of the composite-containing ice crystals can be observed (Table 2).

**Table 2. Analysis of the Stress–Strain Curves and Some Parameters Derived from the MR Equation**

sample designation	$C_1$	$C_2$	cross-link density ( $\nu$ ) mol/cm <sup>3</sup>
dry at RT (20 °C)	0.05302	0.226	$4.35 \times 10^{-5}$
20 days at RT (20 °C)	0.04316	0.0336	$3.54 \times 10^{-5}$
dry at -20 °C	0.06034	0.5131	$5.73 \times 10^{-5}$
20 days at -20 °C	0.06711	0.5946	$6.38 \times 10^{-5}$

The increase in the cross-link density indicates a larger number of rubber chains forming a network structure with ice crystals (acting as cross-linking points) through hydrogen bonding.

To understand how the reinforcing character of the ice crystals is developed during the transformation of water to ice, the storage modulus of the dry sample and of the water-swollen elastomer was measured as a function of time with a constant static and dynamic load at -20 °C and is shown in Figure 5a. The modulus of the dry rubber is almost unaltered with time. However, the increase in the storage modulus is remarkable when the composite was swollen with water (20 days). This increase in the storage modulus can be used to visualize the formation of ice crystals with time.

The strain sweep analysis was carried out at -20 °C to evaluate the dependence of storage modulus on dynamic strain and is shown in Figure 5b. In general, the storage modulus of the unfilled composites was expected to be independent of dynamic strain, whereas the filled composites exhibited a nonlinear dependence of storage modulus on dynamic strain, which can be attributed to the destruction of the filler–filler network, the so-called Payne effect.<sup>23</sup> Hereby, it was found that the higher the volume fraction of ice crystals formed inside of the rubber, the stronger the Payne effect. On the other hand, it is important to note that this effect is negligible for the dry GECO sample. This confirms the filler networking of ice crystals inside of the water-swollen GECO composite. The strain dependencies of the water-swollen elastomers were analyzed by means of the phenomenological model by Kraus,<sup>24</sup>

which is based on the agglomeration–deagglomeration mechanism of the fillers

$$\frac{E'(\gamma) - E'_\infty}{E'_0 - E'_\infty} = \frac{1}{1 + (\gamma/\gamma_c)^{2m}} \quad (9)$$

Hereby,  $E'(\gamma)$  is the modulus of the composite at the strain  $\gamma$ ,  $E'(\gamma) = E'_\infty$  at very large strain;  $E'(\gamma) = E'_0$  at very low strain  $\gamma_0$ ;  $\gamma_c$  is the critical strain at which the magnitude of  $E'_0 - E'_\infty$  becomes half; and  $m$  is a constant (strain sensitivity of the mechanism of filler–filler contact breakage), which depends on specific fractal dimensions of the fractal agglomerate structures of the fillers. The parameter  $\gamma_c$  is largely dependent on the nature and type of the fillers and polymers and the state of the dispersion of the filler in the soft elastomer matrix. The values of  $\gamma_c$  and  $m$  are shown in Table 3. It can be found that  $\gamma_c$  is

**Table 3. Strain Sweep Analysis of the Water-Swollen Elastomers at -20 °C: Values Derived from the Kraus Model**

sample (days)	critical strain, $\gamma_c$ (%)	exponent, $m$
2	3.67	1.58
7	3.62	1.01
20	3.85	0.79

almost similar, indicating the similar type of rubber–filler and filler–filler interactions. However, the value of  $m$  decreases with the increase in the water content of the rubber. There have been some reports on the  $m$  value of typical carbon black-filled rubber composites, and it is found that the value of  $m$  is independent of the type and nature of the carbon black and is constant at  $\sim 0.6$ .<sup>25</sup> In our present case, the value of  $m$  is not a constant, indicating that the ice crystals formed at different levels of water content might have different morphologies and crystal structures.

Figure 6a shows the attenuated total reflection Fourier transform infrared (ATR-FTIR) spectra of dry and 20-day water-swollen GECO composites, measured at RT. The spectroscopic distinction of composites before and after water exposure is quite clear and obvious. The ATR-FTIR spectrum of 20-day water-swollen elastomers shows typical intensive broad bands of both stretching and deformation vibrations of the water hydroxyl group at 3415 and 1639 cm<sup>-1</sup>,

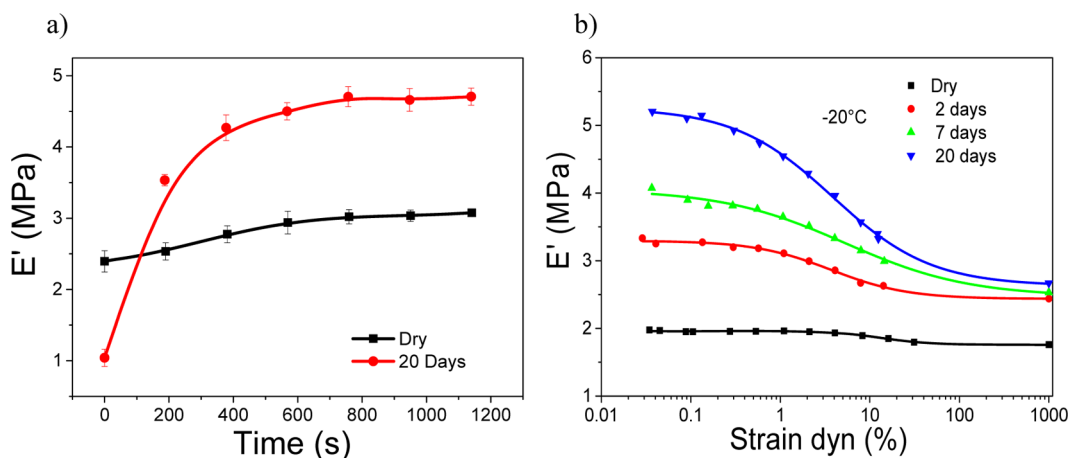


**Figure 5.** (a) Time sweep of dry and 20-day water-swollen elastomers (dynamic strain—1%; static strain—0.2% at -20 °C). (b) Storage modulus  $E'$  as a function of dynamic strain. Data for high strains are extrapolated for hydrodynamic reinforcement from the unfilled GECO. Solid dots and lines represent experimental values and fitted curves, respectively.

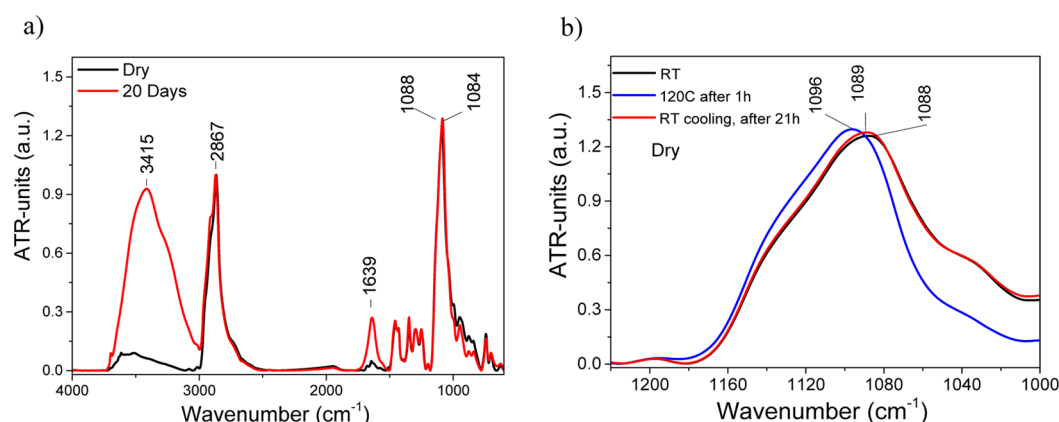


**Figure 6.** ATR-FTIR analysis/spectra of GECO composites: (a) dry and 20-day water-swollen elastomers and (b) ATR-FTIR spectra at room and elevated temperatures: dry composite at RT, after 1 h treatment at 120 °C, after cooling back to RT, and after 21 h at RT.

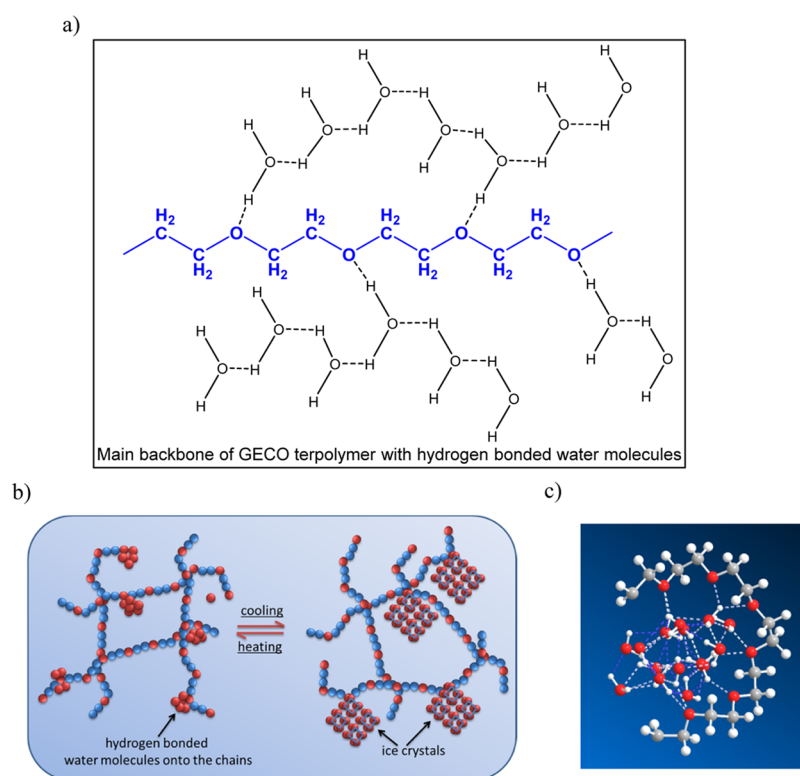


**Figure 7.** (a) Hydrogen-bonding interaction with water molecules and polymer chains, (b) schematic representation of the rubber–filler interaction, and (c) molecular dynamics simulation of the polymer and some water molecules (red—oxygen atom, gray—carbon atom, and white—hydrogen atom).

respectively,<sup>26</sup> indicating a high water concentration in 20-day water-swollen GECO composites.

According to the chemical structure of GECO, one would expect intermolecular hydrogen bonding between ether groups and water molecules (Figure 6a), usually resulting in a band shift of a corresponding bonded structure in an infrared spectrum. Taking into account such a behavior, the ATR-FTIR spectrum of the 20-day water-swollen elastomers (Figure 6a) should have a remarkable band shift of the ether group (band of asymmetrical stretching vibration of the ether group at 1088  $\text{cm}^{-1}$ <sup>26</sup> in the spectrum of the initial dry sample) to lower frequencies after water penetration into GECO. However, only a weak shift of the ether band has been noticed [4  $\text{cm}^{-1}$  band movement (to 1084  $\text{cm}^{-1}$  after water exposure)], which is close

to the spectrum resolution and can hardly be used as a reliable sign of ether–water interaction.

On the other hand, the functionalities of the GECO polymer are known to be quite polar in nature; therefore, a prominent hydrogen bonding and the corresponding band movement would be highly expected. Therefore, it is important to note that in the ATR-FTIR spectra in Figure 6a, the dry (nonswollen) composites show medium to weak bands in characteristic spectroscopic water regions as well (3415 and 1639  $\text{cm}^{-1}$ ), which indicates the presence of moisture in the dry GECO composites. (To understand the moisture absorption behavior of the dry composites, water absorption of dry composites at RT for 20 days was characterized and was found to be 1.5%.)

To confirm the hydrogen-bonding interaction between the ether groups of GECO and water molecules, temperature-dependent ATR-FTIR spectroscopy was performed. The initial dry specimen was heated up to 120 °C and was cooled down back to RT (see Experimental Section for details) to avoid the presence of moisture. The particular ATR-FTIR spectra are presented in Figure 6b. As expected, after temperature treatment, a remarkable band shift of the ether group (to higher frequencies, 8  $\text{cm}^{-1}$ ) is observed, pointing out the interaction of ether groups with moisture (absorbed due to the hydrophilic nature of GECO). Cooling down the system back to RT, the reversibility of band shift can be observed. After 21 h in air at RT, the ether band moved back to lower frequencies (7  $\text{cm}^{-1}$ ). The fact is that the ether groups in the initial dry sample have already been “busy” (bonded) with water molecules (moisture) absorbed from air, which explains the weak movement of ether bands regardless of the amount of water in the 20-day water-swollen elastomers.

Figure 7a describes the possible hydrogen bonding between the polymer chains (ether group) and the water molecules (hydrogen group) along with some free water molecules. The proposed mechanism of water-swollen elastomers at different temperatures is shown in Figure 7b: when the composite is cooled, the freezable water molecules form ice crystals, which are already weakly-hydrogen-bonded with polymer chains.

To visualize the possible molecular arrangement of the polymer chains and water molecules, molecular dynamics simulations were performed (ChemBio3D 14.0, Perkin-Elmer, MM2 optimization). A polymer molecule with 7 polyoxyethylene repeating units was taken along with 15 water molecules and simulated. Hereby, it was observed that the polymer chain encloses a cluster of water molecules, which indicates a strong hydrophilic character of the polymers (Figure 7c).

## CONCLUSIONS

Hydrophilic, cross-linked GECO elastomers can absorb water; at low temperatures, part of the absorbed water can act as reinforcing filler, when the water is frozen into ice crystals. A detailed mechanistic study was carried out, and for the first time, the reinforcing nature of ice crystals in soft elastomers was explored. Direct stress–strain experiments and a sharp reduction in the  $\tan \delta$  peak heights in DMA experiments very clearly indicate the reinforcing character of solid ice crystals. Although a large amount of water can be absorbed by the cross-linked rubber, only a part of these absorbed water molecules (~74% of the total water) can be converted into ice crystals. The size of the ice crystals remains in the submicron range of 400–700 nm. Obviously, these submicron ice crystals formed inside of the rubber are directly linked with polymer chains by weak hydrogen bonding with oxygen atoms present in the GECO polymer. Thus, this direct polymer/filler interaction leads to the reinforcement of the GECO composites. As the solid–liquid phase transition of water takes place at higher temperature range (~0 °C), more specifically at the temperature range higher than the glass transition temperature of the polymer, this kind of material can be used for mechanically adaptable applications, where the material will behave in different ways (hard or soft) depending on the temperature, while maintaining its elastic nature, that is, more than 1500% stretchability with lower and higher stiffness. The findings of this work can also inspire the design of smart

adaptive tires with situation-controlled, ice-grip, wet-skid, rolling-resistance, and other dynamic properties.

## EXPERIMENTAL SECTION

**Materials.** The polyether-based GECO elastomer (Hydrin T3108) was obtained from Zeon Chemicals. It is a terpolymer of epichlorohydrin (CO), ethylene oxide (EO), and allyl glycidyl ether (AGE) (Figure 8). This terpolymer contains 18–

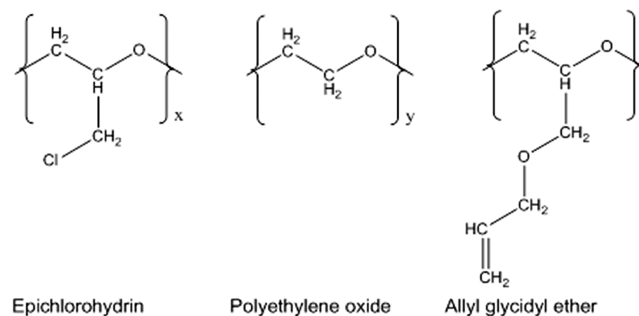


Figure 8. Chemical structure of GECO.

20% of chlorine (epichlorohydrin), 6–8% of double bonds (AGE), and a high amount of EO. The density of GECO is 1.28  $\text{g}/\text{cm}^3$ ; its glass transition temperature is  $-51$  °C (material supplier's data, from DSC measurements). The other compounding ingredients used were of rubber grade. This terpolymer can be cross-linked by sulfur or peroxide because of the presence of AGE in the terpolymer. The cross-linking chemicals sulfur, zinc oxide (ZnO), stearic acid, 2-mercapto-benzothiazole, and 3-methylthiazolidone-2-thione used were of rubber grade.

**Composite Preparation.** The rubber mixture was compounded in an internal mixer (Haake Rheomix, Thermo Electron GmbH, Karlsruhe, Germany). At first, the GECO and the other ingredients are blended at a fixed rotor speed of 60 rpm and at a temperature of 60 °C. The total mixing time was 10 min. Finally, the compounded mass was removed from the mixer and sheeted out in a two-roll mill (Polymix 110L, Servitech GmbH, Wustermark, Germany) at 70 °C. The optimum cure time ( $t_{90}$ ) of the compound was measured in a moving die rheometer at 160 °C and at a frequency of 1.67 Hz (SIS V-50, Scarabeus GmbH, Germany). The prepared rubber compounds were cured under pressure at 160 °C using  $t_{90}$  value in a hot press.

**Characterization.** Water absorption studies were carried out by immersing the sample in deionized water at RT. At first, the weight of the dry sample was recorded ( $W_d$ ). Then, the sample was immersed in water. The weight of the water-swollen sample was measured ( $W_s$ ) after removing the surface water by blotting with a filter paper, at different times until equilibrium swelling was reached. The water-swelling ratio was calculated by  $(W_s - W_d)/W_d \times 100$ . The temperature sweep analysis was carried out using a rectangular specimen ( $10 \times 2 \times 35$   $\text{mm}^3$ ) using a dynamic mechanical thermal analyzer (Gabo Qualimeter, Ahlden, Germany, Eplexor 150N) in tension mode. The isochronal frequency used was 10 Hz, and the heating rate was 2 K/min with a dynamic load of 0.2% strain and static load at 0.5% strain. Tensile tests were performed using a Zwick 1456 instrument (model 1456, Z010; Ulm, Germany) with a crosshead speed of 200 mm/min (DIN 53504). The tensile samples were exposed to  $-20$  °C for 0.5 h, and then the tensile



tests were carried out at  $-20\text{ }^{\circ}\text{C}$ . Time sweep and strain sweep analyses were carried out using a dynamic mechanical thermal analyzer (Gabo Qualimeter, Ahlden, Germany, Eplexor 2000N) in the tension mode with a rectangular specimen ( $10 \times 2 \times 35\text{ mm}^3$ ). Time sweep analysis was performed with a dynamic load of 0.2% strain and static load at 1% strain, and the measurement was carried out as soon as the temperature of the chamber reached  $-20\text{ }^{\circ}\text{C}$  as a function of time (20 min). Strain sweep analysis was carried out as a function of dynamic load from 0.01 to 30% with 40% static strain, and the sample is exposed to  $-20\text{ }^{\circ}\text{C}$  for 15 min before the measurement.

FTIR spectroscopic analysis was performed using an evacuated Vertex 80v FTIR spectrometer (Bruker, Germany) equipped with an MCT detector and a Golden Gate Diamond ATR unit (attenuated total reflection, SPECAC). ATR-FTIR spectra of dry (nonswollen) and water-swollen elastomers were recorded within the range of  $4000\text{--}600\text{ cm}^{-1}$  at RT. To confirm the hydrogen-bonding interaction between the ether groups of GECO and the water molecules, temperature-dependent ATR-FTIR spectroscopy was performed. The dry GECO sample was heated to  $120\text{ }^{\circ}\text{C}$  and was held for about 1 h, until the water bands in the ATR-FTIR spectrum disappeared. After that, the sample was cooled down back to RT and held for about 21 h to allow the penetration of reversible water vapor into the dry GECO samples. Every spectrum was obtained with  $4\text{ cm}^{-1}$  spectral resolution and 100 scans per spectrum. Before comparison, the spectra were normalized onto the stretching vibration band of the methylene group around  $2867\text{ cm}^{-1}$  (internal reference approach<sup>27</sup>).

For transmission electron microscopy, a piece of water-swollen specimen was cooled down to  $-160\text{ }^{\circ}\text{C}$ , mounted on an ultramicrotome chamber (Ultracut UC7, Leica Microsystems GmbH, Germany), which was flooded with dry nitrogen at a temperature of  $-160\text{ }^{\circ}\text{C}$ . Approximately 120 nm-thick sections with dimensions of  $100 \times 150\text{ }\mu\text{m}^2$  were cut with a diamond knife (temperature of the knife  $-160\text{ }^{\circ}\text{C}$ ) and transferred onto a cooled TEM grid. The grid was transferred under liquid nitrogen into a cryo-TEM holder (Gatan 626, Gatan Inc., USA) and inspected in TEM at  $-170\text{ }^{\circ}\text{C}$ .

## AUTHOR INFORMATION

### Corresponding Author

\*E-mail: [stoeckelhuber@ipfdd.de](mailto:stoeckelhuber@ipfdd.de) (K.W.S.).

### ORCID

Klaus Werner Stöckelhuber: 0000-0003-4237-3617

Amit Das: 0000-0002-2579-1369

### Notes

The authors declare no competing financial interest.

## ACKNOWLEDGMENTS

The authors are thankful to Holger Scheibner for performing stress–strain measurements, Liane Häussler for discussions regarding DSC measurements, and René Jurk for his technical assistance.

## REFERENCES

- (1) Voet, A. Reinforcement of elastomers by fillers: Review of period 1967–1976. *J. Polym. Sci., Part D: Macromol. Rev.* **1980**, *15*, 327–373.
- (2) Heinrich, G.; Klüppel, M.; Vilgis, T. A. Reinforcement of elastomers. *Curr. Opin. Solid State Mater. Sci.* **2002**, *6*, 195–203.
- (3) Mikkelsen, R. L. Using hydrophilic polymers to control nutrient release. *Fert. Res.* **1994**, *38*, 53–59.

- (4) Otsuka, H.; Nagasaki, Y.; Kataoka, K. PEGylated nanoparticles for biological and pharmaceutical applications. *Adv. Drug Delivery Rev.* **2003**, *55*, 403–419.

- (5) Blasi, P.; D'Souza, S. S.; Selmin, F.; DeLuca, P. P. Plasticizing effect of water on poly(lactide-co-glycolide). *J. Controlled Release* **2005**, *108*, 1–9.

- (6) Ito, S.; Hashimoto, M.; Wadgaonkar, B.; Svizero, N.; Carvalho, R. M.; Yiu, C.; Rueggeberg, F. A.; Foulger, S.; Saito, T.; Nishitani, Y.; Yoshiyama, M.; Tay, F. R.; Pashley, D. H. Effects of resin hydrophilicity on water sorption and changes in modulus of elasticity. *Biomaterials* **2005**, *26*, 6449–6459.

- (7) Pouchlý, J.; Biroš, J.; Beneš, S. Heat capacities of water swollen hydrophilic polymers above and below  $0\text{ }^{\circ}\text{C}$ . *Macromol. Chem. Phys.* **1979**, *180*, 745–760.

- (8) Tanaka, M.; Hayashi, T.; Morita, S. The roles of water molecules at the biointerface of medical polymers. *Polym. J.* **2013**, *45*, 701–710.

- (9) Ping, Z. H.; Nguyen, Q. T.; Chen, S. M.; Zhou, J. Q.; Ding, Y. D. States of water in different hydrophilic polymers—DSC and FTIR studies. *Polymer* **2001**, *42*, 8461–8467.

- (10) Bjerrum, N. Structure and properties of ice. *Science* **1952**, *115*, 385–390.

- (11) Kumai, M. Hexagonal and cubic ice at low temperatures. *J. Glaciol.* **1968**, *7*, 95–108.

- (12) Li, W.; Xue, F.; Cheng, R. States of water in partially swollen poly(vinyl alcohol) hydrogels. *Polymer* **2005**, *46*, 12026–12031.

- (13) Ostrowska-Czubenko, J.; Gierszewska-Drużyńska, M. Effect of ionic crosslinking on the water state in hydrogel chitosan membranes. *Carbohydr. Polym.* **2009**, *77*, 590–598.

- (14) Estroff, L. A.; Leiserowitz, L.; Addadi, L.; Weiner, S.; Hamilton, A. D. Characterization of an organic hydrogel: A cryo-transmission electron microscopy and X-ray diffraction study. *Adv. Mater.* **2003**, *15*, 38–42.

- (15) Ahmad, M. B.; Huglin, M. B. DSC studies on states of water in crosslinked poly(methyl methacrylate-co-n-vinyl-2-pyrrolidone) hydrogels. *Polym. Int.* **1994**, *33*, 273–277.

- (16) Rosenberg, R. Why is ice slippery? *Phys. Today* **2005**, *58*, 50.

- (17) Kietzig, A.-M.; Hatzikiriakos, S. G.; Englezos, P. Physics of ice friction. *J. Appl. Phys.* **2010**, *107*, 081101.

- (18) Hsiao-Sheng, C.; Acrivos, A. The effective elastic moduli of composite materials containing spherical inclusions at non-dilute concentrations. *Int. J. Solids Struct.* **1978**, *14*, 349–364.

- (19) Domurath, J.; Saphiannikova, M.; Ausias, G.; Heinrich, G. Modelling of stress and strain amplification effects in filled polymer melts. *J. Non-Newtonian Fluid Mech.* **2012**, *171*, 8–16.

- (20) Mark, J. E. Experimental determinations of crosslink densities. *Rubber Chem. Technol.* **1982**, *55*, 762–768.

- (21) Pradhan, S.; Costa, F. R.; Wagenknecht, U.; Jehnichen, D.; Bhowmick, A. K.; Heinrich, G. Elastomer/LDH nanocomposites: Synthesis and studies on nanoparticle dispersion, mechanical properties and interfacial adhesion. *Eur. Polym. J.* **2008**, *44*, 3122–3132.

- (22) Morris, M. C. Network characterization from stress–strain behavior at large extensions. *J. Appl. Polym. Sci.* **1964**, *8*, 545–553.

- (23) Payne, A. R.; Whittaker, R. E. Low strain dynamic properties of filled rubbers. *Rubber Chem. Technol.* **1971**, *44*, 440–478.

- (24) Kraus, G. Swelling of filler-reinforced vulcanizates. *J. Appl. Polym. Sci.* **1963**, *7*, 861–871.

- (25) Heinrich, G.; Klüppel, M. Recent Advances in the Theory of Filler Networking in Elastomers. In *Filled Elastomers Drug Delivery Systems*; Springer Berlin Heidelberg: Berlin, 2002; pp 1–44.

- (26) Socrates, G. *Infrared and Raman Characteristic Group Frequencies: Tables and Charts*; John Wiley & Sons: New York, 2004.

- (27) Koenig, J. L. *Spectroscopy of Polymers*, 2nd ed.; Elsevier Science: New York, 1999.